Online supplement

Case histories

Proband 1, a 16-year old New Zealand Maori woman, presented with hirsutism and secondary amenorrhea since age 13-years, following menarche at 11-years. She was born to non-consanguineous parents with low birth weight (1300 grams) at term. Her estranged father was reported to have a slim stature and muscular appearance whereas her mother was overweight with a normal body fat distribution. Physical examination revealed hirsutism (Ferriman-Gallway score of 17) and moderate acanthosis nigricans in the neck and axillae. Pubertal development was complete (Tanner stage 5 for breast and pubic hair). Body mass index (BMI) was 23.7 kg/m² and a paucity of subcutaneous fat was apparent in her limbs and trunk. Biochemical investigations revealed diabetes mellitus, severe insulin resistance, dyslipidaemia, elevated liver enzymes and hyperandrogenism (Table 1). Pelvic and abdominal ultrasound showed the presence of polycystic ovaries and hepatic hyper-echogenicity consistent with steatosis. Dual-energy x-ray absorptiometry was consistent with the clinical impression of partial lipodystrophy (DEXA, Table 1).

Given these clinical and biochemical findings, DNA from the patient, her mother (her father was estranged and not available for DNA testing) and an unaffected sibling was sequenced for mutations in *LMNA* and *PPARG*. *LMNA* sequencing was wildtype but a heterozygous Arg308Pro (R308P) *PPARG* mutation was present in the proband but not in her mother or sibling.

Proband 2, a South African woman, presented at age 20-years to a dermatologist with severe acanthosis nigricans. She was found to have polycystic ovarian syndrome and

developed significant congestive cardiac failure at age 21-years. At this point cardiac investigation suggested a dilated cardiomyopathy. Following hospital admission at age 22-years with pancreatitis, she was noted to have severe hypertriglyceridaemia and diabetes. Her father was thought to have had type 2 diabetes mellitus (T2DM) and ischaemic heart disease but was divorced from the proband's mother and estranged from the family. Her mother was clinically unaffected and her brother, aged 24-years, was lean (BMI 22 kg/m^2) and asymptomatic, though biochemical testing later revealed significant hyperinsulinaemia during an oral glucose tolerance test.

In addition to signs of cardiac failure including congestive hepatomegaly, examination revealed extensive acanthosis nigricans, hirsutism and partial lipodystrophy, with reduced limb fat. Biochemical tests revealed insulin-resistant diabetes, labile dyslipidaemia, elevated liver enzymes and hyperandrogenism (Table 1).

LMNA sequencing was wildtype but *PPARG* sequencing identified a novel heterozygous Ala261Glu (A261E) mutation, which was also present in her sibling but not her mother.

Proband 3, a South African woman developed T2DM and hypertension in her early thirties. She also reported hirsutism and oligomenorrhoea. She did conceive subsequently and presented in pregnancy with pancreatitis secondary to severe hypertriglyceridaemia. Her brother, aged 39-years, was also known to have T2DM, severe hypertriglyceridaemia (48.9 mmol/L) and had experienced episodes of pancreatitis. His BMI was 27.5 kg/m^2 and lipodystrophy had not been noted clinically.

On examination, Proband 3, was found to have acanthosis nigricans, hirsutism and partial lipodystrophy.

PPARG sequencing in Proband 3 and her brother also revealed the A261E receptor mutation. Their parents were not available for assessment. This family is not known to be related to that of Proband 2, though both families reside in the same geographical region of South Africa.

Supplementary material

Protein expression and purification. The wild type and mutant PPARγ ligand binding domain (amino-acids 204-477) proteins were cloned into pGEX2T (GE Healthcare) with a TEV site instead of a thrombin site. The proteins were expressed in Rosetta (DE3) (Novagen). Cells were grown at 37° C in 2xTY until $OD_{600nm} = 0.1$, induced with 40 μM Isopropyl-D-1-thiogalactopyranoside (IPTG) followed by overnight growth at 20°C. The bacterial cells were lysed by sonication in a buffer containing 1x PBS, 1% Triton X-100, 5% glycerol, 1 mM Dithiothreitol (DTT) and Complete EDTA-free protease inhibitor (Roche). The soluble protein was bound to glutathione sepharose (GE healthcare), and washed with a buffer containing 1x PBS, 1% Triton X-100, 5% glycerol, 1 mM DTT. Then the bound protein was washed with TEV cleavage buffer containing 25 mM Tris/Cl pH 7.5, 50 mM NaCl, 5% glycerol and 2 mM DTT. The wild type and mutant proteins were eluted from the resin using TEV protease.

Circular Dichroism (CD). For the circular dichroism experiments, the concentration of WT and mutant PPARγ proteins was 33 μM in 25 mM Tris/Cl pH 7.5, 50 mM NaCl, 5% glycerol and 2 mM DTT. For the melting curves, circular dichroism was monitored

at 222 nm, with data points collected as the sample temperature was increased from 10 to 90° C (1° C/min) using a Applied Photo Physics Chirascan plus spectropolarimeter with a Quantum North West temperature controller. A melting temperature was obtained by fitting the data to a 6 parameter thermal unfolding curve using GraphPad Prism.

Nuclear magnetic resonance (NMR) studies. For the NMR experiments the wild type and R308P mutant proteins were further purified by gel filtration in 25 mM Tris/Cl pH 7.5, 50 mM NaCl, 5% glycerol and 2 mM DTT on a Superdex S-200 column (GE Healthcare). Both proteins were buffer exchanged into a buffer suitable for NMR containing 20 mM KH_2PO_4 pH7.4, 50 mM KCl and 1 mM DTT using a PD10 disposable column (GE Healthcare).

All NMR spectra were acquired from 500 μl samples (150 μM protein and 200 μM ligand) with 5% D2O and 1% DMSO-d6 at 25°C on an 800MHz Bruker Avance II spectrometer with cryogenically cooled coldhead. A total of 64 transients were recorded for each experiment, with acquisition times of 70 msec, a 1.5 sec relaxation delay and solvent suppression being achieved using an excitation sculpting scheme (1). Data was zero filled to 8K points and a sinebell squared shifted by 72 deg window function applied prior to Fourier transformation.

References.

Hwang, T.L. & Shaka, A.J. Water Suppression That Works. Excitation Sculpting Using Arbitrary Wave-Forms and Pulsed-Field Gradients. J. Magn. Reson. 1995; 112A, 275-279.

Supplementary Table 1. Summary of clinical features, responses to thiazolidinedione therapy and structural modelling of all FPLD3 mutations

identified in patients whose response to TZD therapy has been - or is reported herein.

Mutation (reference)	WT	P495L (9)		V318M (9)		Y383X (14)		H477L (15)		R308P		A261E	
Gender		female		female		female		female		female		female	
Metabolic features		severe		severe		mild		mild		severe		severe	
Non-alcoholic fatty liver disease		+		+		+		+		+		+	
TZD therapy (duration months)		rosiglitazone (6)		rosiglitazone (6)		pioglitazone (5)		pioglitazone (36)		pioglitazone (24)		rosiglitazone (2)	
	Reference range	start	end	start	end	start	end	start	end	start	end	start	end
Fasting glucose (mmol/l)	N<5.5	10.0	9.3	9.6	7.2	14.4	NR	4.1	NR	12	3.7	6.4	NA
Triglycerides (mmol/l)	N<1.7	5.7	6.3	4.5	6.9	66.4	7.3	2.02	Similar	13.2	1.6	39	10
HDL cholesterol (mmol/l)	N>1.0	0.58	0.79	0.58	0.52	NR	NR	1.16	Similar	0.4	0.7	0.5	NA
Alanine aminotranferase (units/l)	N<35	85	82	39	58	21	NR	29	Improved	64	33	20	NA
HbA1c (%)	4.3<N<6.1	8.7	5.6	7.3	7.1	12.1	7.3	8.4	5.7	7.7	5	16	8
Functional data													
Response to ligand	In vivo	Initial response not sustained		partial response not sustained		Good response stopped due to fluid retention		Good response		Good response		Good response, stopped due to congestive cardiac failure	
	In vitro	no		no		nd		nd		Only high affinity ligands		Only high affinity ligands	
Structural modelling		Mutation destabilises helix 12 which mediates transcriptional activation and is therefore predicted to respond submaximally to any ligand		Mutation destabilises helix 12 mediates transcriptional activation and is therefore predicted to respond submaximally to any ligand		Mutation truncates ligand binding domain, preventing ligand binding so overall response depends on ligand-dependent transcriptional activation of PPARγ derived from wild type allele		Mutation perturbs binding of PGJ2 and rosiglitazone with His 477 but binding of pioglitazone is not predicted to be affected. *		See results		See results	
Melting temperature (ºC) of PPARγ mutant in circular dichroism studies**	46.7	48.6		47.7		ND		ND		46.8		38.0	

N, normal; ND, not determined; NR, not reported; HDL, high density lipoprotein. *See supplementary figure 4; ** See supplementary figure 5.

Supplementary figure legends

Supplementary figure 1. Structures of the ligand binding domain of PPARγ with no ligand (1PRG) (**A**) or bound to Rosiglitazone (2PRG) (**B**), Pioglitazone (2XKW) (**C**), Farglitazar (1FM9) (**D**) or PGJ2 (2ZK1) (**E**). In each structure, the location of mutated residues (A261, R308) together with the different positions adopted by a loop (Cyan) Helix 2 and Helix 3 which could be stabilised by some ligands that bind in the vicinity (**B, C, F**), is highlighted.

Supplementary figure 2. One-dimensional proton NMR spectra of wild-type (top) and R308P mutant (bottom) ligand binding domains in the presence (magenta) and absence (cyan) of Pioglitazone. In both the amide and methyl regions there are characteristic changes associated with Pioglitazone binding. These include a general sharpening of the spectra (particularly evident in the amide region) and new peaks in both the methyl and amide regions around 0.1ppm and 6.05ppm respectively (arrowed). These data demonstrate that both the wild-type and mutant ligand binding domains are able to bind the Pioglitazone ligand.

Supplementary figure 3. Triglyceride (TG) and HbA1C values in Proband 2 without or during rosiglitazone therapy. Proband 2 was treated with rosiglitazone titrated up to 4 mg twice daily on two occasions approximately 18 months apart. On each of these occasions, TZD use was prompted by significant deteriorations in her metabolic control. On both occasions fasting TG and HbA1c levels fell (more strikingly for HBA1c than TG) during rosiglitazone treatment, but worsening pre-existing congestive cardiac failure necessitated drug withdrawal.

Supplementary figure 4. Crystallographic modelling based on structures of unliganded PPARγ (1PRG) or bound to PGJ2 (2ZK1), to rosiglitazone (2PRG) or pioglitazone (2XKW). (**A**) P495 is situated at the beginning of helix 12; the P495L mutation will destabilise the position of helix 12 regardless of ligand occupancy. (**B**) V318 is orientated towards helix 12;

V318M mutation will also destabilise the position of helix 12 regardless of ligand occupancy. **(C)** Comparison of the position of H477 in the ligand binding pocket with different ligands reveals direct interaction with rosiglitazone and PGJ2, but not pioglitazone. **(D)** The H477L mutation disrupts the interaction with rosiglitazone and PGJ2, whereas it is not predicted to affect pioglitazone binding.
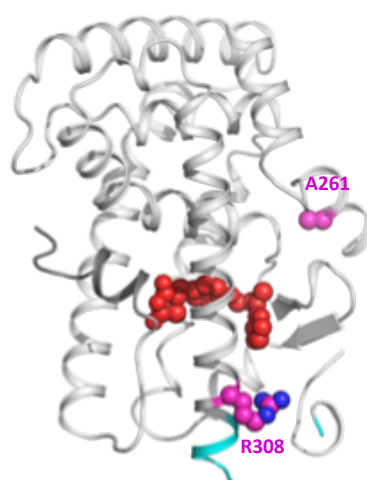
Supplementary figure 5. Circular dichroism (CD) thermal denaturation curves of wild type (WT) or mutant PPARγ ligand binding domains showing that the A261E receptor mutation destabilises the conformation of the LBD.
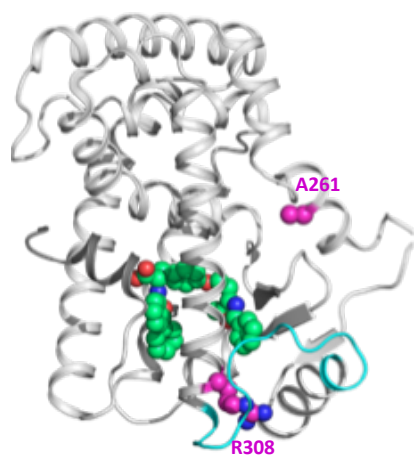
Supplementary Figure 1
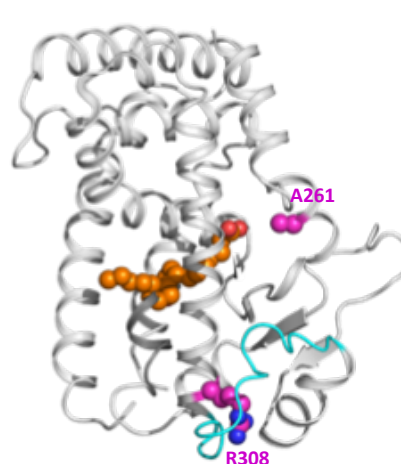
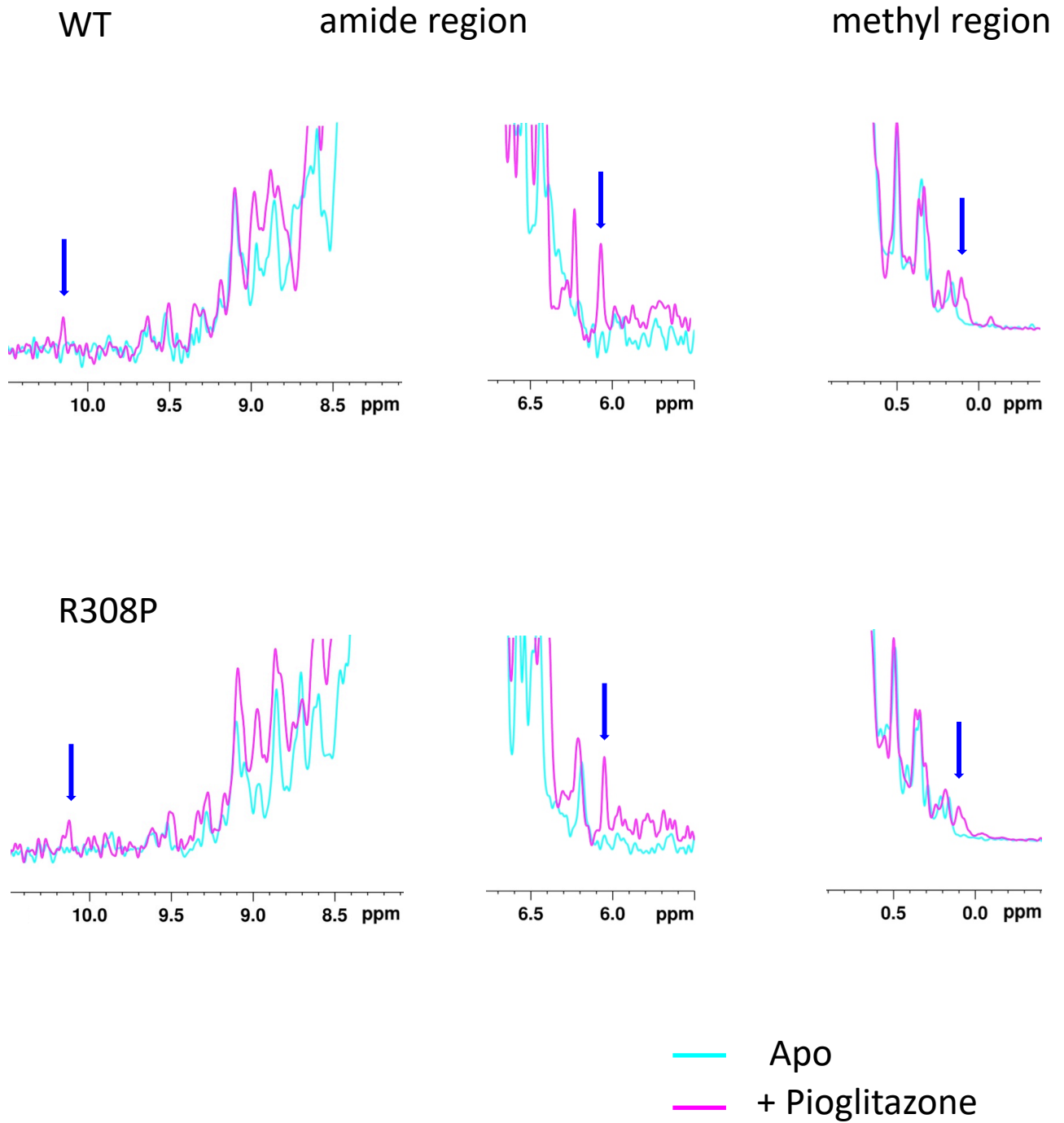**A** Unliganded
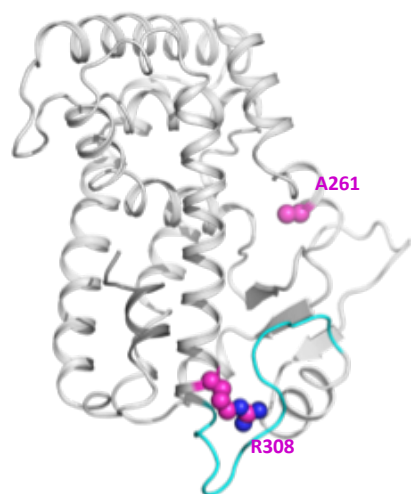
B Rosiglitazone

C Pioglitazone
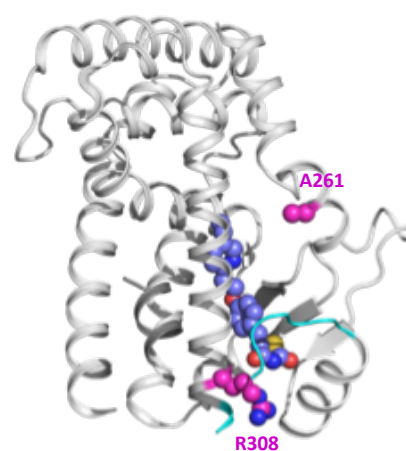
D Farglitazar

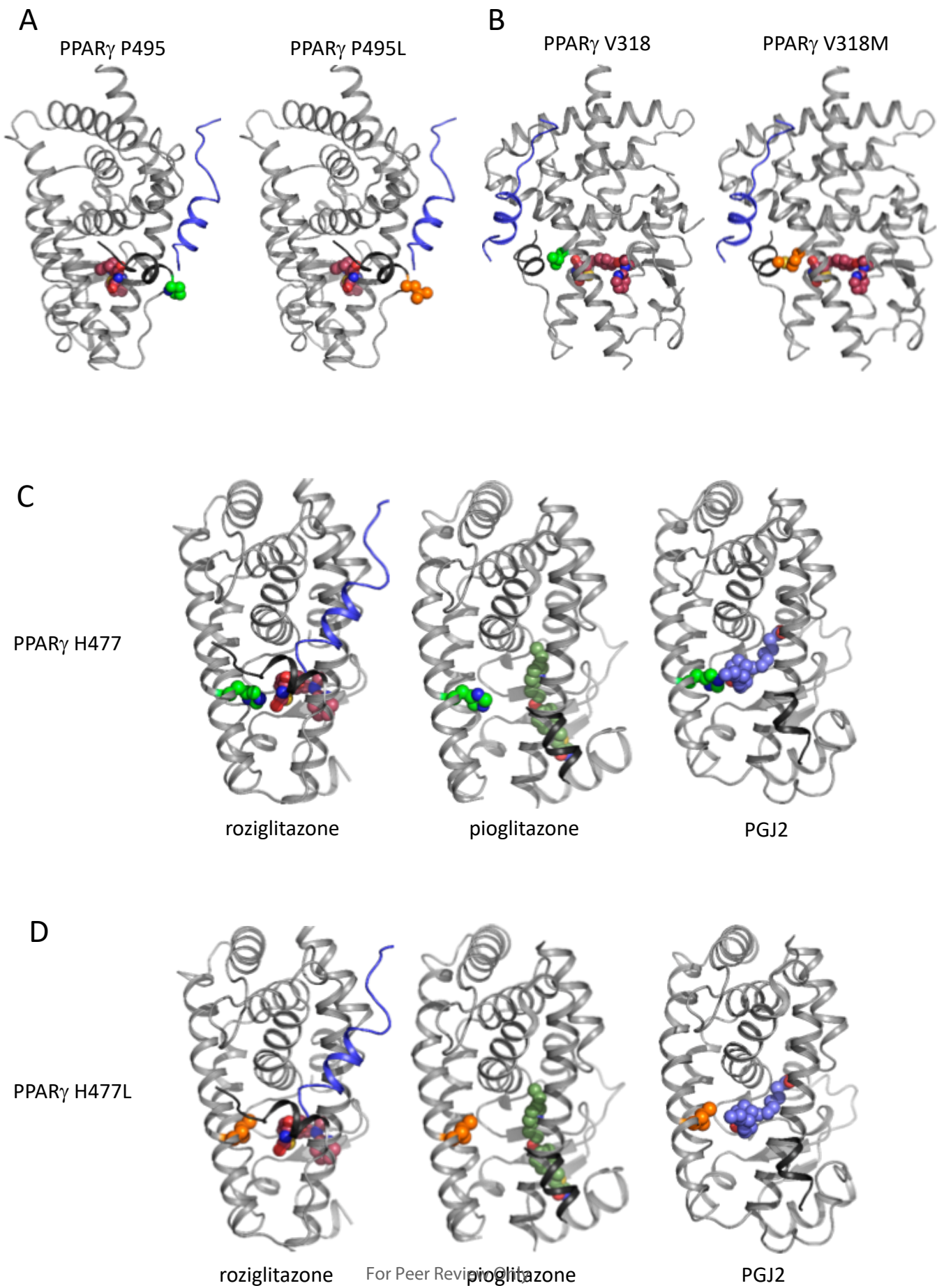**E** PGJ2

Supplementary Figure 2

Supplementary Figure 3

Supplementary Figure 4

A

PPARγ P495   PPARγ P495L

B

PPARγ V318   PPARγ V318M

C

PPARγ H477

roziglitazone   pioglitazone   PGJ2

D

PPARγ H477L

roziglitazone   For Peer Review pioglitazone   PGJ2

Supplementary Figure 5